ISSN 1069-3513, Izvestiya, Physics of the Solid Earth, 2011, Vol. 47, No. 2, pp. 137–145. © Pleiades Publishing, Ltd., 2011.
Original Russian Text © Yu.F. Moroz, T.A. Moroz, 2011, published in Fizika Zemli, 2011, No. 2, pp. 64–73.

Numerical 3D Modeling of the Magnetotelluric Field in Kamchatka

Yu. F. Moroz and T. A. Moroz

Institute of Volcanology and Seismology, Far Eastern Branch, Russian Academy of Sciences, bul'v. Piip 9, Petropavlovsk–Kamchatskii, 683006 Russia

Received

Abstract—We consider the key features in the responses of magnetic tippers and MTS curves to the sharp contrast in electric conductivity at the interface between the land and the sea waters of the Sea of Okhotsk and the Pacific bounding Kamchatka. The zones with different intensity of the coast effect are revealed. Stronger manifestations of the effect are found to occur in the East Kamchatka, which is related to the induction effects of the electric currents concentrated in the Kuril–Kamchatka trench. Indentation of the coastline resulted in the appearance of three-dimensional (3D) effects in the magnetotelluric field of the eastern Kamchatka. These effects in the variations of the geomagnetic field are vanishing with an increasing period, giving room to low-frequency effects in the MT field, which are associated with the flow of electric currents around Kamchatka (the around–flow effect). It is shown that the transverse MTS curves over the entire region of Kamchatka suffer from the *S* effect at low frequencies and do not characterize the deep geoelectric structure. Only in the middle segments of the West and Central Kamchatka, the longitudinal MTS curves are weakly subjected to the induction effects and thus reflect the distribution of the deep electric conductivity. On the eastern coast of Kamchatka both the longitudinal and transverse MTS curves are strongly distorted by the 3D effects caused by the abundant capes and bays. The interpretation of MTS data in this region should necessarily invoke the 3D modeling of an MT field.

DOI: 10.1134/S1069351311010071

INTRODUCTION

Being located in the zone of transition from the mainland to the Pacific, Kamchatka has a complex geological structure. The deep distribution of the electric conductivity in this region is studied using the magnetotelluric and magnetovariational sounding methods (MTS and MVS, respectively). The interpretation of the sounding data is fraught with the difficulties associated with the effects of geoelectric inhomogeneities, primarily, with the sharp contrast in the electric conductivity at the interface between the inland surface layer and the sea water in the Sea of Okhotsk and the Pacific. This contrast, usually measuring three to four orders of magnitude, manifests itself in the coast effect. The situation is complicated by the fact that the east coast of Kamchatka on the Pacific side has a very indented coastline divided into numerous capes and bays. Various effects arising here hamper the interpretation of MTS–MVS curves.

Earlier, we made an attempt to apply the techniques of physical and numerical thin-sheet modeling to study the influence of the upper inhomogeneous layer on the pattern of the magnetotelluric fields [Moroz and Kobzova, 1994]. However, due to the limitations inherent in the physical and thin-sheet modeling, only simplified models were used in these works, and the results obtained did not provide a comprehensive idea of the behavior of MT and MV curves. Therefore, we invoked 3D numerical modeling of the magnetotelluric field for the study of the coast effect. The present paper addresses the results of this research.

1. THE 3D MODEL OF KAMCHATKA AND THE STRATEGY OF NUMERICAL MODELING

Modeling of the MT field in Kamchatka was based on the bathymetry map presented in Fig. 1. In the region of the west coast of Kamchatka (in the water area of the Sea of Okhotsk) the sea depths attain 7 km. In this region, the deep Kuril–Kamchatka trench runs along the Pacific coast of Kamchatka and extends by almost 700 km. In its northwestern part, the Kamchatka trench adjoins the Aleutian trench. In the context of geoelectrics, Kamchatka is a northwest elongated 3D inhomogeneous structure with a maximum width of 430 km. In the northeast it narrows to 100 km, forming the so called Kamchatka isthmus; in the south, it ends by an acute tip. The western coastline of Kamchatka is smooth, and only the small Utkholok peninsula is prominent here. The eastern coastline is very indented; it is divided into the Govena, Il'pinskii, Ozernoi, Kamchatskii, Kronotskii and Shipunskii capes separated by bays.

The 3D geoelectric model of Kamchatka has the following parameters. In order to ensure estimation of the coast effect separately from the influence of the geoelectric inhomogeneities contained in the sedimentary–volcanic cover of Kamchatka, the thickness

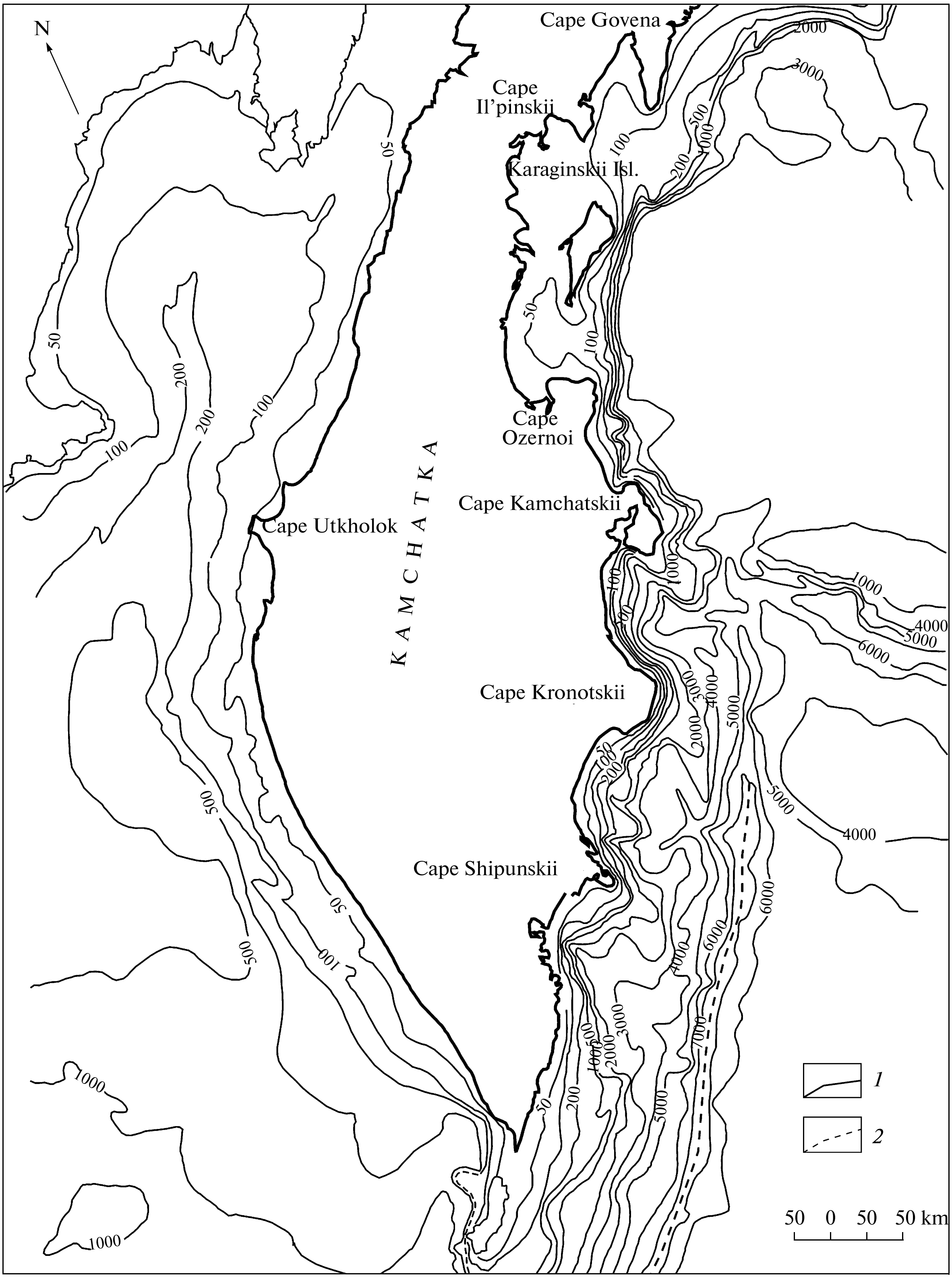

Fig. 1. Bathymetric map of the Kamchatka water area: *1* the isobaths, *2* the axis of the deep Kuril–Kamchatka trench.

and the electric resistivity of the upper inland layer are assumed to be constant. The inland surface layer has a thickness of 3 km and a resistivity of 30 Ω m, which are the approximately average values yielded by the electromagnetic studies of Kamchatka [Moroz, 1991]. The electric resistivity of the sea water is 0.25 Ω m. The deep geoelectric cross section is standard [Rokityanskii, 1975; Moroz, 1994]. Vertical thicknesses of the model layers (from top to bottom) are 0.1, 0.2, 0.2, 1.5, 1, 1, 1, 1, 80, 120, 100, 100 and 300 km.

The model calculations were carried out using the known Mackie program [Mackie et al., 1994]. The *X* and *Y* grid axes were oriented along and across Kamchatka, respectively. The entire grid is composed of 150 elements on the *Y* and 60 elements on the *X* axes. The size of the grid cell was 10 × 10 km; in the region with very indented coastline the grid was densified, and the size of the cell was 5 × 5 km. Such a grid density was selected in view of the further use of the grid in the calculations of the test models with an inhomogeneous upper inland layer. The sizes of the marginal grid cells were tens, hundreds, and thousands of times larger to ensure the two-dimensionality and one-dimensionality of the boundary conditions, which allowed us to considerably speed up the convergence of the iterative process. Computations were conducted for 25 periods ranging from 1 s to 2500 s. For each segment of the model, we calculated the frequency curves of the magnetic tipper, the real and imaginary parts of the induction matrix (tipper), the real and imaginary induction arrows, apparent resistivity curves, and phase curves of the impedance along the *Y* and *X* axes. These results were compared with the data of earlier 3D modeling of north Kamchatka [Moroz and Nurmukhamedov, 2004]. The discrepancy in the electric parameters was found to be at most 5%, which indicates fairly high accuracy of the model calculations.

2. THE ANALYSIS OF THE MAGNETOVARIATIONAL SOUNDING DATA

Let us recall the important features of the magnetotelluric parameters [Berdichevsky and Zhdanov, 1981; Vozoff, 1972; Schmucker, 1970; Wiese, 1965; Parkinson, 1959]. The basic magnetovariational relation is

$$H_z = H_{zx}H_x + W_{zy}H_y,$$

where $\mathbf{W} = |W_{zx}, W_{zy}|$ | is the magnetic tipper; H_z, H_x, and H_y are the components of the geomagnetic field; W_{zx}, W_{zy} are the matrix components that depend on frequency, on the distribution of electric conductivity in the Earth, and on the orientation of the coordinate axes.

The components of the induction matrix determine the induction arrows:

$$\mathrm{Re}\mathbf{W} = \mathrm{Re}\,W_{zx}\,1_x + \mathrm{Re}\,W_{zy}\,1_y,$$

$$\mathrm{Im}\mathbf{W} = \mathrm{Im}\,W_{zx}\,1_x + \mathrm{Im}\,W_{zy}1_y.$$

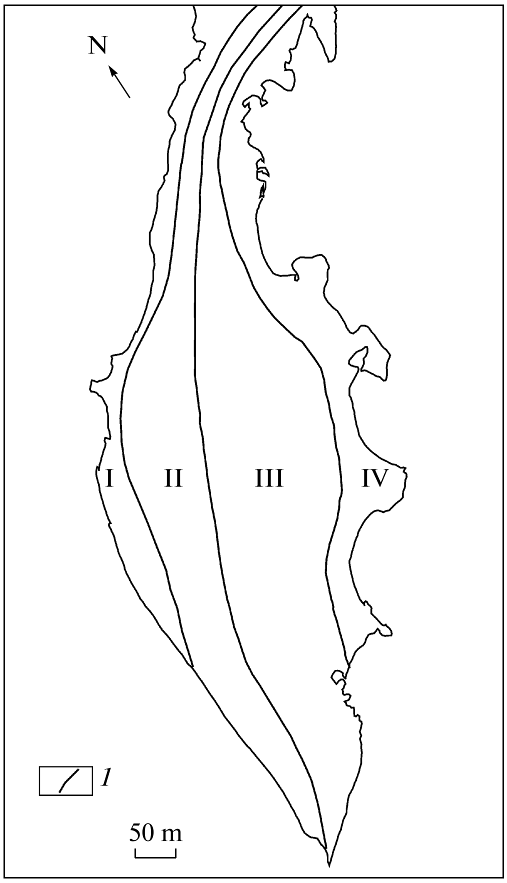

Fig. 2. The zones characterized by different intensity of the coast effect in the frequency curves of magnetic tipper in Kamchatka: @1 the boundaries of the zones.

The frequency curves for tipper, induction arrows, and their azimuths describe the pattern of the coast effect over the territory of Kamchatka. Consider the frequency curves **ReW**. According to their shapes, these curves are classified into 4 groups corresponding to zones with different intensities of the coast effect. The revealed zones and typical tipper curves for each zone are shown in Figs. 2 and 3.

Zone I is located offshore in the Sea of Okhotsk. Here the real and imaginary arrows at short periods (at most 200 s) point seawards to the Sea of Okhotsk. At periods of 400–500 s the real induction arrow has a well-expressed maximum attaining 0.45. The maximum in the magnitude of the real induction arrow corresponds to the minimum in the imaginary induction arrow, and the latter changes its azimuth by 180°. These peculiarities in the behavior of the arrows are quite typical in 2D inhomogeneous models. The maximum in $|\mathrm{Re}\mathbf{W}|$ is associated with the saturation by the electric current of the sea water at the shelf of the Sea of Okhotsk. At low periods the real and imaginary arrows become noncollinear due to the influence of the large 3D geoelectric inhomogeneity, to which the southern tip of Kamchatka can probably be related.

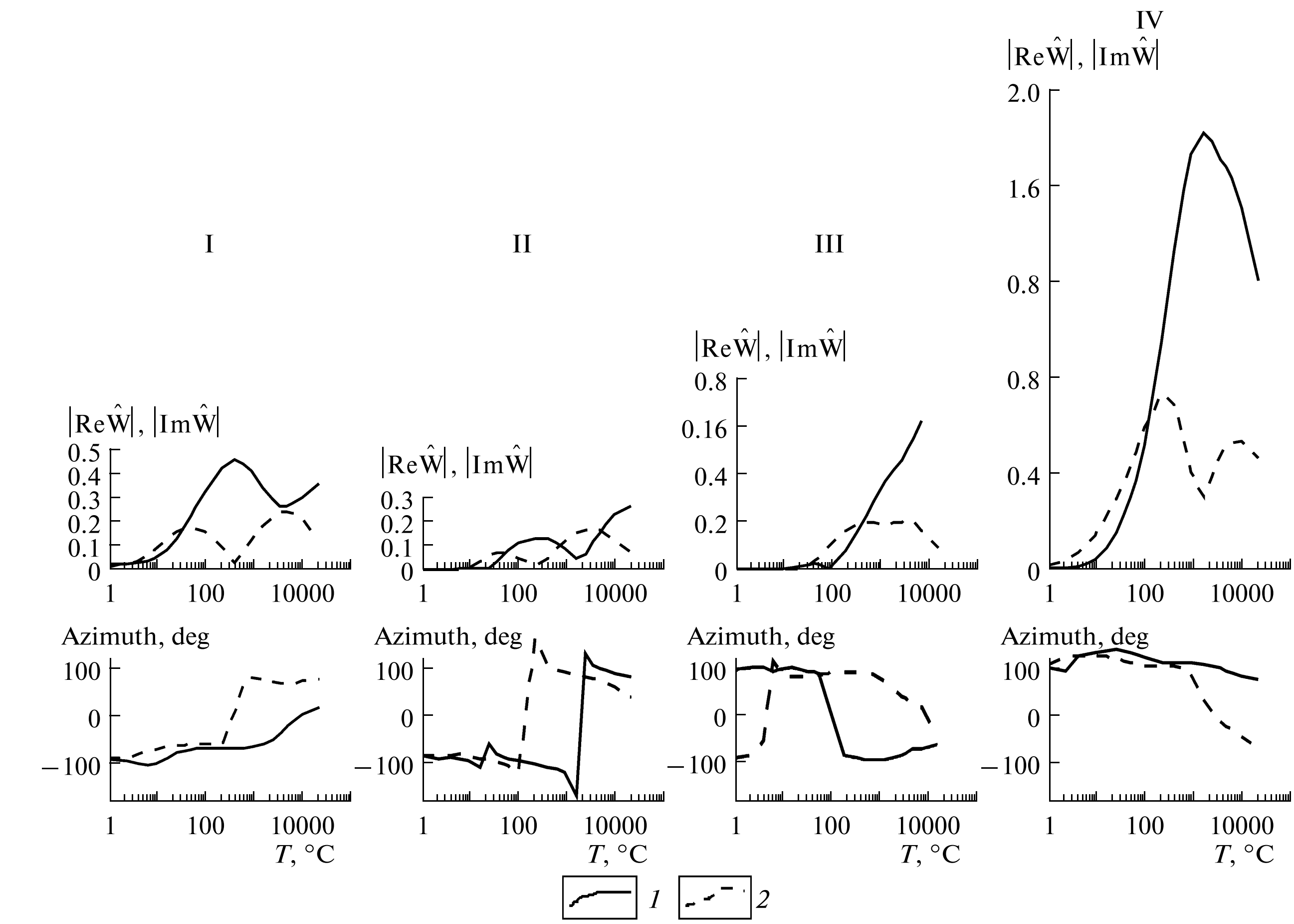

Fig. 3. Typical frequency curves of the magnetic tipper for the zones in Fig. 2: @1 and @2 the curves of the magnitudes and the azimuths of the real and imaginary induction arrows.

Zone II lies to the east of zone I. Here the curve of the real arrow magnitude has a maximum at the periods of 400–500 s, although in absolute value this maximum is one-third the maximum in zone I. The maximum in |**ReW**| in zone II corresponds to the minimum in the |**ImW**| curve, as in zone I. At high frequencies (periods below 100 s), the real and imaginary induction arrows are collinear and point towards the Sea of Okhotsk. It is worth noting that in the low-frequency band the magnitude of the real arrow increase and its orientation changes by 180° so that the arrow points towards the Pacific. These features indicate that the coast effect on the side of the Sea of Okhotsk becomes weaker, while the sea electric currents induced in the Pacific Ocean begin coming into effect.

Zone III is located to the east of Zone II. Here, the |**ReW**| curve, represented by an ascending asymptotic branch, lacks a maximum caused by an influence of the sea current in the Sea of Okhotsk. The |**ImW**| curve has a maximum and a descending branch. The lacking maximum in the |**ReW**| frequency curve at periods of 400–500 s and the presence of the ascending branch at low frequencies are indicative of the overall attenuation of the coast effect on the side of the Sea of Okhotsk and its considerable strength on the side of the Pacific.

Zone IV relates to the east coast of Kamchatka, which includes numerous capes and bays. The curve of the magnitude of the real induction arrow has a well-pronounced maximum at periods of 1000–2000 s. This maximum is associated with the saturation by the electric current of the deep trench extending along the Pacific coast of Kamchatka. The magnitudes of the real induction arrow attain 1.8 at the maximum, which indicates a strong coast effect. The maximum in the magnitude of the real arrow corresponds to the minimum in the imaginary arrow, accompanied by the change in its azimuth by almost 130° At low frequencies the angle between the real and the imaginary arrows increases to 120°. These features revealed in the behavior of the frequency curves of the magnetic tipper show that in Zone IV 2D effects prevail in the geomagnetic field up to periods of 1000–2000 s. With an increasing period of variations, 3D effects, which are likely due to the limited southern extension of Kamchatka, start to develop.

A better visualization of the coast effect is provided by the sketches showing the behavior of the induction

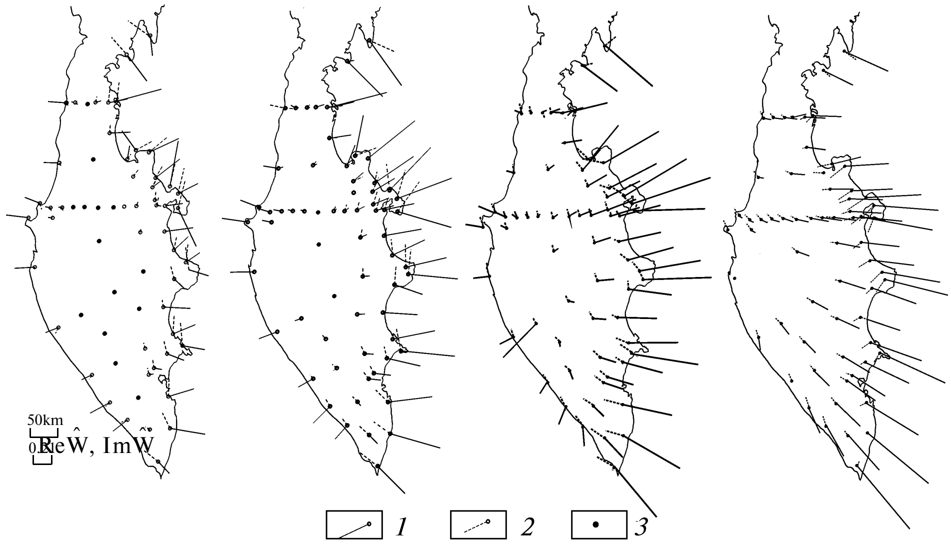

Fig. 4. The behavior of the induction arrows at the periods (*a*) 100 s, (*b*) 400 s, (*c*) 1600 s, and (*d*) 10000 s: *1* and *2* the real and the imaginary induction arrows, respectively; *3* the sites where the vectors are close to zero.

arrows at periods of 100, 400, 1600, and 10000 s (Fig. 4). At a period of 100 s, the coastal effect appears in the zones near the shore of the Sea of Okhotsk and the Pacific. In the middle segment of Kamchatka the coast effect is barely manifested at all. On the west coast, the induction arrows exhibit a regular pattern of orientation towards the Sea of Okhotsk. On the east coast, the orientations of the real and the imaginary arrows change due to the very indented coastline. In most cases the angle between the arrows differs from 0 and 180°, and the lengths of the imaginary arrows are commensurable to the lengths of the real arrows, indicating the presence of 3D effects.

At a period of 400 s, the area influenced by the coast effect expands. Only in the central part of Kamchatka there is an intact narrow zone where the coast effect has no impact. On the west coast, the behavior of the induction arrows remains practically similar to that observed at a period of 100 s. In the zone near the shore on the east coast of Kamchatka, the real arrows are noticeably longer than the imaginary arrows, showing the induction effect of the active electric current in the Pacific.

At a period of 1600 s, the coast effect spreads over almost the entire territory of Kamchatka. The real and the imaginary induction arrows associated with the coast effect increase in the middle part of the peninsula. The west coast remains under the influence of the electric currents flowing in the Sea of Okhotsk. On the east coast, the real arrows increase their magnitudes, becoming many times larger than the imaginary arrows. This shows that the coast effect strengthens due to the concentration of the electric currents in the deep trench.

At a period of 10000 s, the coast effects becomes stronger. It spans over the major part of Kamchatka. In the southwestern part of the peninsula the induction arrows point towards the deep trench in the Sea of Okhotsk. On the east coast the influence of the indented coastline dies out.

Towards the inland Kamchatka the coast effect becomes weaker. What is the nature of this attenuation? According to [Rokityanskii, 1975], the weakening of the coast effect is the sum of the geometric attenuation and the absorption in the conductive medium. The geometric attenuation is proportional to the distance to the source that is a certain elongated stripe of anomalous currents concentrated in the sea water. The geometric attenuation results in the reduction of the magnitude of the real induction arrow, although it does not affect the shape of the frequency response. This is clearly seen in the example of curves in zones I and II up to a period of 2000 s, since at larger periods the coast effect in zone II starts influencing on the side of the Pacific. The absorption manifests itself in the high-frequency range, which results in the shifting of the maximum of the frequency curve towards the longer periods. Thus, in zone IV the maximum in the frequency response of the magnitude of the real arrow appears at 2000 s, whereas towards the inland Kamchatka (zone III) the maximum is not as distinct because it falls beyond the considered interval of periods.

Let us see how the coast effect is influenced by the increase in the electric conductivity of the lithosphere of Kamchatka. To study this issue, we introduced a layer with reduced electric resistivity at a depth of 15 km into the initial model characterized by the standard distribution of the deep electric conductivity. The thickness of the conductive layer is 20 km, and the electric resistivity is 10 Ω m. Computations showed that introduction of the layer with a conductivity of

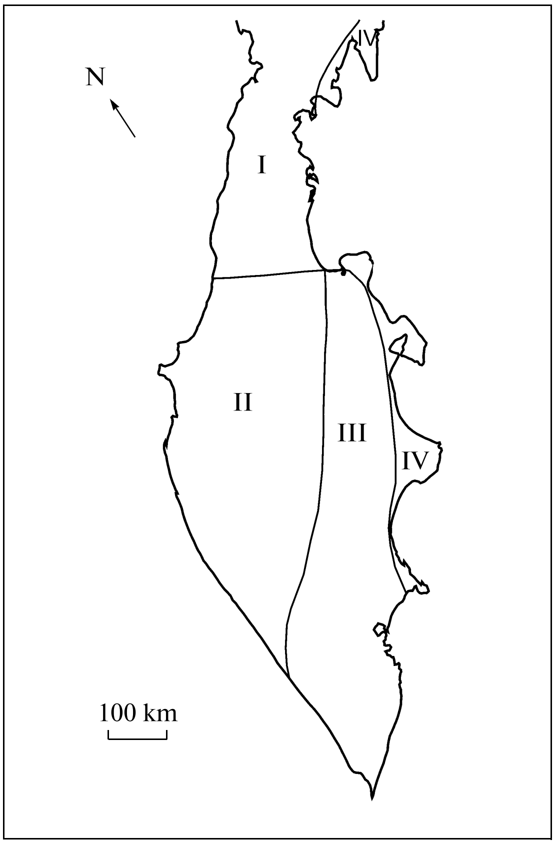

Fig. 5. The regions of Kamchatka with different intensity of the coast effect in the MTS curves.

2000 S into the lithosphere of Kamchatka results in the severalfold reduction in |Re**W**| and |Im**W**|. This is an important indication of large conductive zones beneath Kamchatka.

3. THE ANALYSIS OF THE MAGNETOTELLURIC SOUNDING CURVES

The numerical modeling provided for each grid node a locally normal MTS curve and MTS curves along and across the strike of Kamchatka, which will further be called the longitudinal and the transverse curves. According to their shapes, the longitudinal and the transverse MTS curves were classified into four groups characterizing different intensities of the coast effect (Fig. 5). These groups correspond to the different regions of Kamchatka (Fig. 6).

The first region includes the northern part of Kamchatka where the peninsula narrows, forming an isthmus. The width of the isthmus is 120 km and the length is 200 km. The transverse amplitude curve contains a minimum and an ascending branch coming to a maximum. The asymptotic branch is dragged into the high-resistivity area, which is due to the *S*– effect caused by the sharp contrast between the onshore and the offshore conductivity. The influence of the *S*–effect appears already at short periods, which is clearly seen in the phase curves. The transverse curve departs from the locally normal curves at periods of 4–5 s. At low periods this curve does not reflect variations in the deep geoelectric structure, and at a period of 10000 s it differs from the locally normal curve (in terms of resistivity) by almost an order of magnitude.

The longitudinal amplitude curve has a descending branch in the low-frequency domain. This curve qualitatively reflects the depth distribution of the electric conductivity. At low frequencies it lies at a lower level of resistivity than the locally normal MTS curve. Such a deviation, amounting a few dozen percent in the region considered, is related to the influence of induction of the sea's electric currents. A noticeable disagreement between the longitudinal and the locally normal amplitude curves starts already at periods of 60–100 s; and the phase curves begin diverging at periods as short as 16–20 s. The longitudinal and the locally normal phase curves merge together at 64000–10000 s; this indicates that the influence of the induction effect on the longitudinal impedance dies out.

Region II is located in the middle of Kamchatka. The transverse amplitude curve has a minimum, an ascending asymptotic branch, and a maximum. At low frequencies the asymptotic branch is "hauled up" in terms of the resistivity level. This is caused by the *S*–effect, which starts at periods of approximately 200–300 s. At these periods the transverse curve noticeably deviates from the locally normal curve. The difference between the curves reaches almost half an order of magnitude at a period of 10000 s. The influence of the *S* effect on the phase curves is apparent at shorter periods of 30–40 s. The deviation of the transverse phase curve is about 15° at 10000 s.

The longitudinal amplitude curve practically coincides with the locally normal one. The difference between the curves is a few percent, which falls within the accuracy of the numerical modeling of the magnetotelluric field. The same also relates to the longitudinal phase curve. Its deviation from the locally normal curve attains 5° only in the low-frequency domain where the accuracy of the phase determination is likely reduced due to the boundary conditions of the model.

Region III includes the southern tip of Kamchatka and has an eastern extension. The transverse amplitude curve has a minimum and an ascending asymptotic branch that flattens out at low frequencies. The distortion of the transverse curve here is again associated with the *S*–effect caused by the contrast in the conductivity at the land–sea water interface. A noticeable influence of the *S*–effect starts from the periods 60–100 s. The deviation of the transverse curve from the locally–normal curve at 10000 s exceeds an order of magnitude. The impact of the *S*–effect on the phase curves is apparent at as short a period as 4 s and grows with an increasing period. The difference between the transverse and the locally normal phase curves at a period of 1000 s amounts up to 20°.

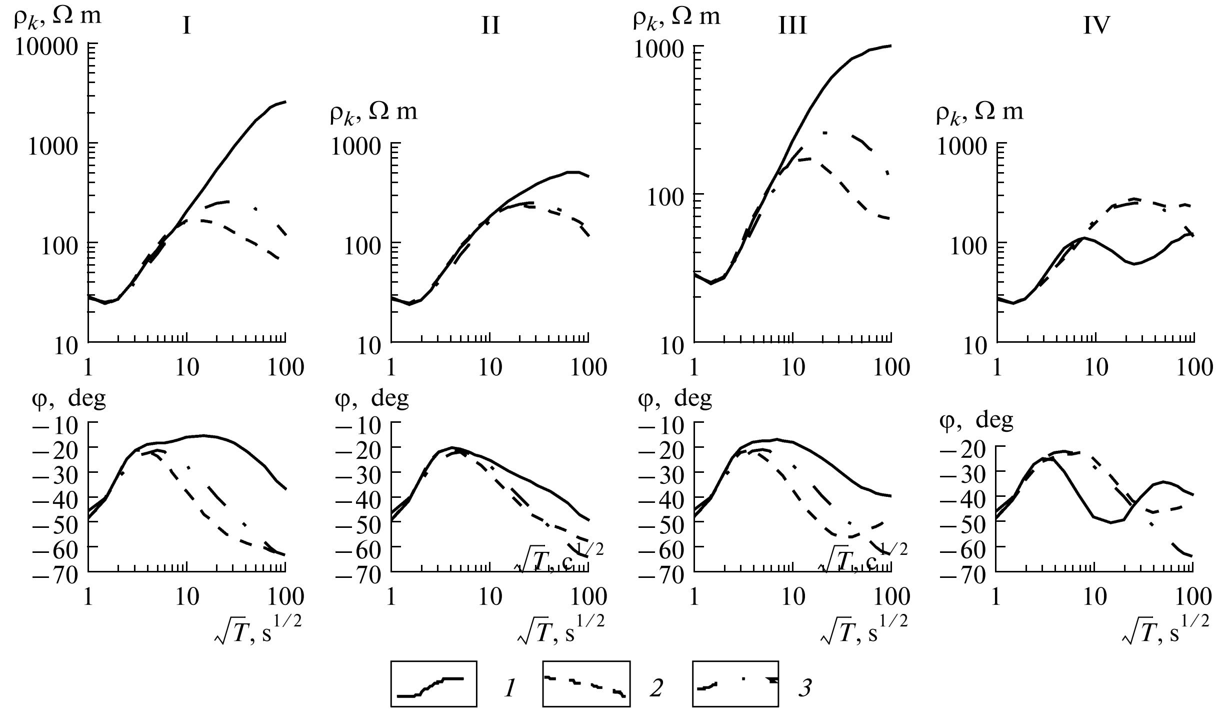

Fig. 6. Typical MTS curves for the regions in Fig. 5. Roman numerals are the numbers of the typical curves corresponding to the regions in Fig. 5. *1*, *2*, and *3* are the transverse, the longitudinal, and the locally normal MTS curves.

In the low-frequency domain, a minimum appears in the longitudinal amplitude curve. This minimum is caused by the induction effect of the electric currents concentrated in the Pacific. The influence of the induction effect becomes apparent at a period of 150–200 s, which is reflected in the deviation of the longitudinal curve from the locally normal one. The maximal difference between the curves reaches approximately 300% at 1600 s. The induction effect starts appearing in the phase curve at a period of 50 s and reaches its maximum at 1000 s. At periods exceeding 1000 s, the longitudinal phase curve has an ascending branch that intersects the locally normal curve. Such behavior of the longitudinal phase curve is likely associated with the southern closing of Kamchatka.

Region IV covers the east capes of Kamchatka, where the coastline is very indented. The electric currents induced in the sea flow around the east capes and give rise to 3D effects that manifest themselves in the longitudinal and the transverse curves. The intensity of these effects depends on where the observations of the MT fields are conducted. Here it is hardly possible to identify a typical longitudinal and transverse MTS curve since the shapes of the curves are very diverse. The induction effect and the *S* effect appear in either the longitudinal or transverse curve, depending on the configuration of the coastline.

The transverse curve, in contrast to the locally normal one, has a distinct minimum at periods 400–2500 s; the minimum in the phase transverse curve appears at periods 64–600 s. The minimum is associated with the induction effect of the electric currents flowing along the boundary of the peninsula, which at this segment is oriented across the strike of Kamchatka. At lower frequencies corresponding to periods of 6400–10000 s, the transverse amplitude curve intersects the locally normal curve, which is also linked with the 3D effects. These peculiarities are better expressed in the phase curves where the maximum in the transverse curve corresponds to the descending branch of a locally normal curve.

The longitudinal amplitude curve coincides with the locally normal curve up to a period of 1600 s. With increasing period the amplitude curve deviates from the locally normal curve and becomes a nearly horizontal asymptotic branch. This disagreement between the curves is more distinct in the behavior of the phase curves. The longitudinal phase curve starts deviating from the locally normal curve at a period of 900 s. At 1000–1500 s, the minimum appears in this curve, which is inconsistent with the descending branch of the locally normal curve. Thus, we arrive at a conclusion that the longitudinal and the transverse MTS curves do not reflect the deep distribution of the electric conductivity. MTS curves in region IV cannot be used for formal interpretation. In order to estimate the parameters of the deep electric conductivity in this region we should invoke 3D numerical modeling.

Consider the model of Kamchatka containing a crustal conductive layer at a depth of 15 km. The thickness of the layer is 20 km and its resistivity is 10 Ω m. The longitudinal and the transverse ampli-

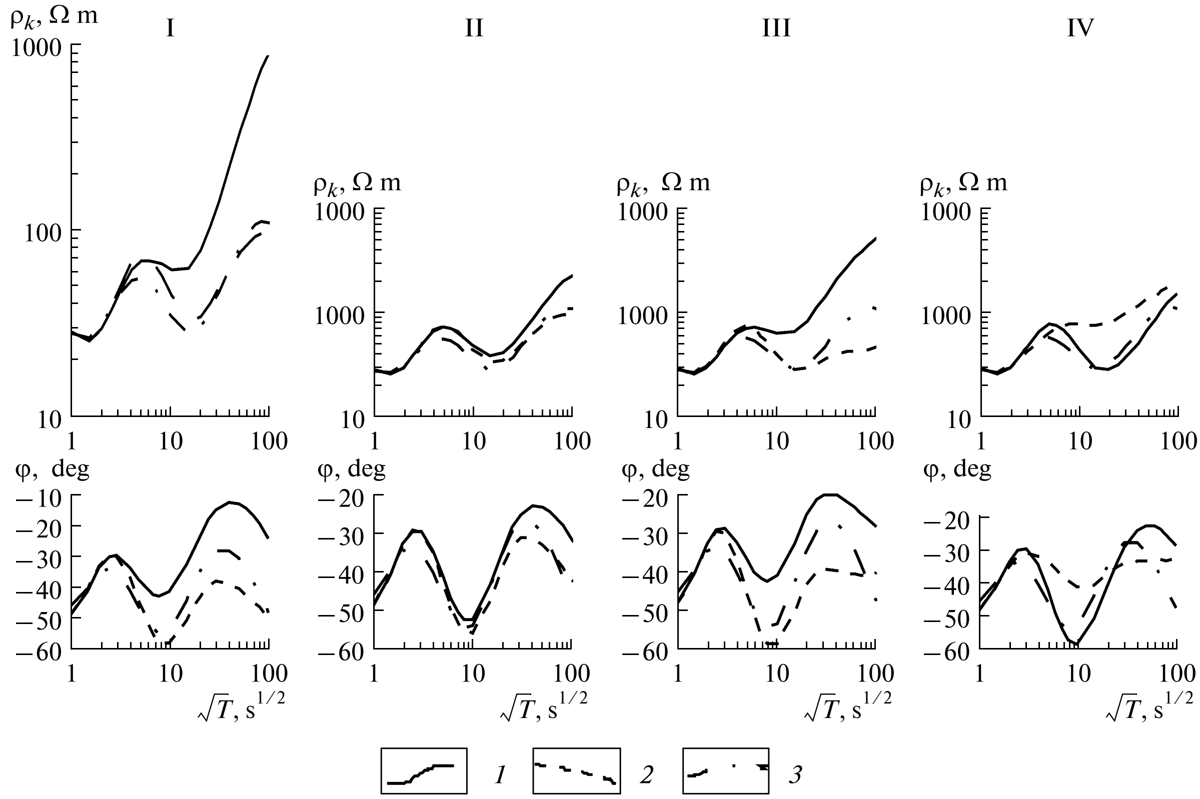

Fig. 7. Typical MTS curves in the model of Kamchatka containing a crustal conductive layer. Roman numerals are the numbers of typical curves corresponding to the regions in Fig. 5. *1*, *2*, and *3* are the transverse, the longitudinal, and the locally normal MTS curves.

tude and phase curves for this model are presented in Fig. 7. Practically all curves show some indications of the crustal layer. Let us consider the patterns of MTS curves in the distinguished regions of Kamchatka. In region I, the crustal layer is less evident in the transverse curve than in the longitudinal one, which is due to the influence of the coast effect. The longitudinal amplitude curve almost coincides with the locally normal one. The induction effect caused by the action of the electric currents in the Sea of Okhotsk, in fact, vanishes against the stronger influence of the electric currents flowing in the crustal conductive layer. Note that the phase longitudinal curve noticeably deviates from the locally normal one at periods 400–800 s, which indicates its higher sensitivity to the induction effect in the region considered.

In region II, where the influence of the coast effect attenuates, the divergence between the transverse and the locally normal curve markedly decreases compared to region I. There are noticeable indications of the coast effect apparent in the transverse amplitude and phase curves only at low frequencies. The longitudinal amplitude and phase curves faintly differ from the corresponding locally normal curves, which is due to the weak induction effect of the electric currents flowing in the Okhotsk Sea and the Pacific.

The coast effect observed in region III is related to the influence of the electric currents in the Pacific. In this region the transverse amplitude curve is similar to its counterpart in region I. The longitudinal amplitude curve at periods ranging from 1 s to 400 s is close to the locally normal curve. At lower frequencies the longitudinal curve differs from the locally normal one due to the induction effect.

In region IV the crustal layer is reflected in both the longitudinal and transverse curves. Indications of this layer are less distinct in the longitudinal curve (for Kamchatka) due to the *S*–effect related to the contrast in conductivity at the interface between the onshore cape Kamchatskii and the sea water. The transverse curve practically coincides with the locally normal one. This shows that the influence of the crustal layer, in fact, suppresses the induction effect of the electric currents.

CONCLUSIONS

1. The coast effect in Kamchatka is associated with the influence of the electric currents concentrated in the Sea of Okhotsk and in the Pacific. The simultaneous induction impact of these currents in the territory of Kamchatka forms a complicated pattern in the behavior of the magnetotelluric parameters. According to the tipper frequency curves, four zones with dif-

ferent intensity of the coast effect are distinguished. On the west coast, the strongest coast effect appears at periods of 400–500 s. Further eastwards, the coast effect on the side of the Sea of Okhotsk vanishes, giving place to the coast effect on the side of Pacific, which strongly increases on the east coast of Kamchatka. The maximum coast effect occurring at the periods of about half an hour is almost four times as intense as the effect on the west coast. The maximum in the coast effect on the west coast of Kamchatka is associated with the saturation of the deep trench by the electric current inducing the vertical component of the magnetic field that strikes through east Kamchatka.

2. The configuration of the domain captured by the coast effect on the side of the Sea of Okhotsk and the Pacific depends on the period of geomagnetic variations. At long periods ($T > 5000$ s) the coast effect on the side of Sea of Okhotsk and the Pacific spreads over the entire territory of Kamchatka. Thus, at a period of 100 s only the middle segment of the peninsula, and at a period of 1600 s, only a narrow (50 km wide) zone in its middle part are free of coast effects.

3. The 3D effects in the variations of the geomagnetic field in Kamchatka have different intensities in different frequency bands. At short periods (below 400 s), the effects are due to the flow–around of the indented coastline by the electric current. These effects decay with increasing period of geomagnetic variations and die out at a period of 10000 s. At the same time, effects related to the flow of an electric current around Kamchatka, which is a 3D extended geoelectric inhomogeneity in the highly conductive sea water, develop over long periods.

4. According to the longitudinal and the transverse (relative to the strike of Kamchatka) MTS curves, four regions with diverse manifestations of the coast effect are distinguished. Over most of the territory of Kamchatka (regions I, II, and III), the transverse MTS curves experience the *S*–effect, which shifts the curves up to a higher level of resistivity. Therefore, the transverse curves are not informative of the depth variations of the electric conductivity. The longitudinal curves in the Kamchatka isthmus (region I) and in region III adjacent to the east capes are distorted by the induction effect caused by the electric currents in the Sea of Okhotsk and in the Pacific. Only in the middle part of the West and Central Kamchatka (region II) the longitudinal curve is free of the induction effect and reflects the depth distribution of conductivity. The east coast of Kamchatka (region IV) is characterized by the complex behavior of the longitudinal and the transverse MTS curves, which is due to the 3D effects associated with the very indented coastline. The induced electric currents flow around the capes and are concentrated in bays. Due to the flow-around and current-gathering effects as well as to the *S* and the induction effects in regions with an elongated coastline of local capes and bays, the MTS curves have diverse shapes depending on the specific location of MT observations. Neither the longitudinal nor transverse MTS curves reflect the deep geoelectric structure of the model. Therefore, the interpretation of MTS curves in this situation should necessarily involve 3D numerical modeling.

5. The presence of a deep conductive layer (with a conductivity of 2000 S) in the geoelectric model of Kamchatka results in a severalfold decrease in the magnetic tipper and noticeable attenuation of the induction effect in the MTS curves. These features are important indications of the deep conductive structures revealed beneath Kamchatka.

6. The main distinctive features in the behavior of the MTS and MVS curves, which are due to the coast effect, are revealed for the model with a uniform inland layer and a uniform deep conductor. The obtained results are important at the first stage of the 3D numerical modeling of the MT field in Kamchatka. Supposedly, further research will address the study of the MT field in the 3D models of Kamchatka, containing an inhomogeneous layer inland and an inhomogeneous deep conductive body in the Earth's crust and mantle. We hope that this work will result in the construction of a 3D model of the electric conductivity distribution deep in the Earth.

REFERENCES

Berdichevskii, M.N. and Zhdanov, M.S., *Interpretatsiya anomalii peremennogo elektricheskogo polya Zemli* (Interpretation of the Anomalies in the AC Electric Field of the Earth), Moscow: Nedra, 1981.

Mackie, K., Smith. J.T. and Madden, T.R., Three-Dimensional Electromagnetic Modeling using Finite Difference Equations: the Magnetotelluric Example, *Radio Sci.*, 1994, vol. 29, no. 4, pp. 923-935.

Moroz, Yu.F. and Kobzova, V.M., Physical and Numerical Modeling of the Magnetotelluric Field of Kamchatka, *Vulkanol. Seismol.*, 1994, no. 2, pp. 86-98.

Moroz, Yu.F. and Nurmukhamedov, A.G., A Deep Geoelectric Model of the Junction Zone

of the Kurile-Kamchatka and Aleutian Island Arcs, *Fiz. Zemli*, 2004, no. 6, pp. 54-67 [*Izv. Phys. Earth* (Engl. Transl.), 2004, vol. 40, no. 6, pp. 502—-514].

Moroz, Yu.F., *Elektroprovodnost' zemnoi kory i verkhnei mantii Kamchatki* (Electric Conductivity of the Earth's Crust and the Upper Mantle in Kamchatka), Moscow: Nauka, 1991.

Parkinson, W.D., Directions of Rapid Geomagnetic Fluctuations, *Geophys. J.*, 1959, vol. 2, pp. 1-14.

Rokityanskii, I.I., *Issledovanie Anomalii Elektroprovodnosti Metodom Magnitovariatsionnogo Profilirovaniya* (Study of the Anomalies in Electric Conductivity using the Magnetovariational Profiling Technique), Kiev: Naukova Dumka, 1975.

Schmucker, U., *Anomalies of Geomagnetic Variations in the South-Western United States*, Berkeley: Univ. California Press, 1970.

Vozoff, K., The Magnetotelluric Method in the Exploration of Sedimentary Basins, *Geophysics*, 1972, vol. 37, pp. 98-141.

Wiese. H., *Geomagnetische Tiefentelluric*, Berlin: Deutsche Akad. Wiss., 1965.